

Electron Transport Properties of Rapidly Solidified $(\text{GeTe})_x(\text{AgSbTe}_2)_{1-x}$ Pseudobinary Thermoelectric Compounds

B. S. Kim,^{1,*} I. H. Kim,² J. K. Lee,² B. K. Min,¹ M. W. Oh,¹ S. D. Park,¹ H. W. Lee,¹ and M. H. Kim²

¹Korea Electrotechnology Research Institute, Changwon-si, Gyeongnam 641-120, Korea
²Changwon National University, Changwon-si, Gyeongnam 641-773, Korea

$(\text{GeTe})_x(\text{AgSbTe}_2)_{1-x}$ ($x = 80, 85$) compounds were fabricated by melting-hot press and RSP-hot press processes. The $(\text{GeTe})_{85}(\text{AgSbTe}_2)_{15}$ compound, which composed of mainly crystalline and partly amorphous structures, was produced in part by rapid solidification. X-ray diffraction analysis showed that the $(\text{GeTe})_x(\text{AgSbTe}_2)_{1-x}$ compounds represented a single phase of GeTe. The electron transport properties were evaluated over the temperature range of RT~773K, and then systematically changed with compositions x in $(\text{GeTe})_x(\text{AgSbTe}_2)_{1-x}$ compounds. The maximum Seebeck coefficient was 227 $\mu\text{V/K}$ at 673K in the $(\text{GeTe})_{80}(\text{AgSbTe}_2)_{20}$ compounds fabricated by melting and hot-press process. The minimum resistivity was shown in the $(\text{GeTe})_{85}(\text{AgSbTe}_2)_{15}$ by melting and hot-press process.

Key words: thermoelectric materials, electron transport properties, rapid solidification process, $(\text{GeTe})_x(\text{AgSbTe}_2)_{1-x}$

1. INTRODUCTION

The recycling of waste heat, which is inevitably produced by every variety of heating system, is a worldwide issue for solving the energy problems. It has been suggested that thermoelectric power generation technology may prove a suitable means for recycling such waste heat. The efficiency of thermoelectric conversion is a direct result of the performance of thermoelectric materials, and can be estimated by the dimensionless figure of merit, $ZT = \alpha^2 / \rho\kappa$, where, α is the Seebeck coefficient ($\Delta V/K$), ρ the electrical resistivity, and κ the thermal conductivity.^[1-3]

Recent studies have sought to reduce thermal conductivity by phonon scattering at the interfaces of nanostructure in the matrix.^[4,5] Recent advances have been reported in PbTe, GeTe, and SnTe compounds for the 500 K to 750 K range, which are similar in both crystal structure and chemical similarity.^[6] In particular, $\text{Pb}_m\text{AgSbTe}_{m+2}$ has shown an excellent figure of merit, $ZT = 1.5\text{--}2.2$, which is due to the embedded nanodots and phase inhomogeneity in the PbTe matrix.^[4,5]

Since the early 1960s, scientists have studied GeTe thermoelectric compounds doped with silver and antimony which is $(\text{GeTe})_x(\text{AgSbTe}_2)_{1-x}$, called TAGS- x in the hopes of power generation in the medium temperature range of 500 K to 800 K. The optimum composition of TAGS- x is $(\text{GeTe})_{85}(\text{AgSbTe}_2)_{15}$, which has proper mechanical stability and thermoelectric

performance ($ZT = 1.4$) compared with $(\text{GeTe})_{80}(\text{AgSbTe}_2)_{20}$, which has good thermoelectric properties ($ZT = 1.9$) but poor mechanical stability.^[7,8] The TAGS compound behaves as a p-type semiconductor, and exhibits low thermal conductivity of 1.2 W/mK due to its microstructural complexity.^[9,10] Recent studies in TAGS compounds have reported how antiphase domains, twin-boundary defects, and nanodomains with different orientations have been affected by manufacturing processes.^[10,11,12]

In this paper we focus on the effect of the presence of a non-crystalline phase in TAGS compounds. We primarily investigated the electron transport properties of rapidly solidified TAGS- x ($x = 80, 85$) compounds.

2. EXPERIMENTAL PROCEDURE

Raw materials of Ge, Te, Ag, and Sb with 5N purity were weighed for $(\text{GeTe})_x(\text{AgSbTe}_2)_{1-x}$ ($x = 80, 85$) with stoichiometry. We used two different processes to fabricate specimens: melting-hot press, which consisted of conventional melting, pulverizing, and hot-pressing and RSP-hot press, which is consisted of melting, rapid solidification process (RSP), pulverizing, and hot-pressing. The mixtures of each raw material were sealed in a carbon-coated quartz ampoule purged with Ar gas after evacuation of 5×10^{-3} Pa, and kept at 1273 K for 10 h. For compositional homogeneity, the ampoules were rocked at 10 RPM during the melting process, and then quenched with water. The as-cast ingots were then pulverized to powder under 325 meshes before being hot-pressed at 773 K with 100 MPa pressure for 1 hour

*Corresponding author: bskim@keri.re.kr

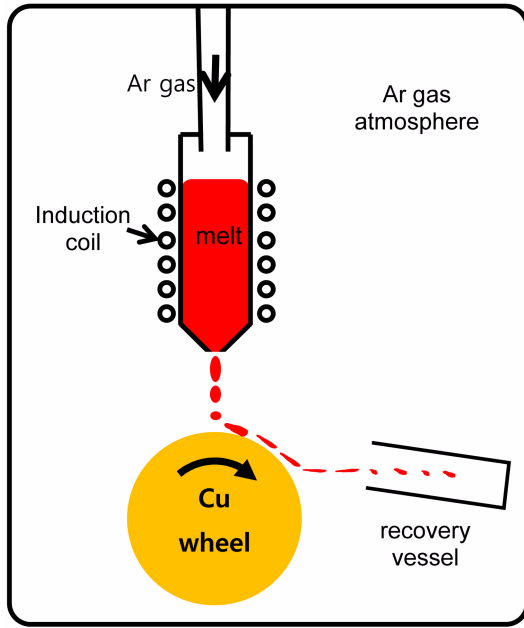


Fig. 1. Schematic diagram of rapid solidification process (RSP).

in an Ar gas atmosphere. The density of the hot-pressed specimens measured by Archimedes method was 97% to 98% relatively compared with theoretical density.

The RSP-hot press process added the step of RSP with melted ingot. The induction-melted specimen was shot to a Cu wheel rotating with a line speed of 40 m/s, which caused it to be solidified into a ribbon with a thickness of a few tens of micrometers. The ribbon of TAGS-85 compound was then pulverized and hot pressed with same condition described as previously. Figure 1 shows the schematic diagram of RSP.

The phase of the hot pressed specimens fabricated by both the melting-hot press and RSP-hot press process was identified by X-ray diffraction peaks with a Cu-K α diffractometer (PANalytical, MPD). The microstructure and selected area electron diffraction (SAED) of rapid solidified TAGS ribbons were investigated with a high resolution transmission electron microscope (JEM 2100, JEOL). The Seebeck coefficient and electrical specific resistivity were measured in the range of room temperature to 773 K with a commercial ULVAC ZEM-3(M10), which is controlled and computer-aided. The Hall coefficient (R_H) was measured at room temperature under 0.7T with a five-probe configuration of ECOPIA HMS-3000 system using a Van der Pauw method.

3. RESULTS AND DISCUSSION

Figure 2 shows the XRD patterns of hot-pressed $(\text{GeTe})_x(\text{AgSbTe}_2)_{1-x}$ ($x = 80, 85$) compounds. The phase of all specimens was a single GeTe phase which is a rhombohedral structure with a space group of $R\bar{3}m(160)$. All peaks of

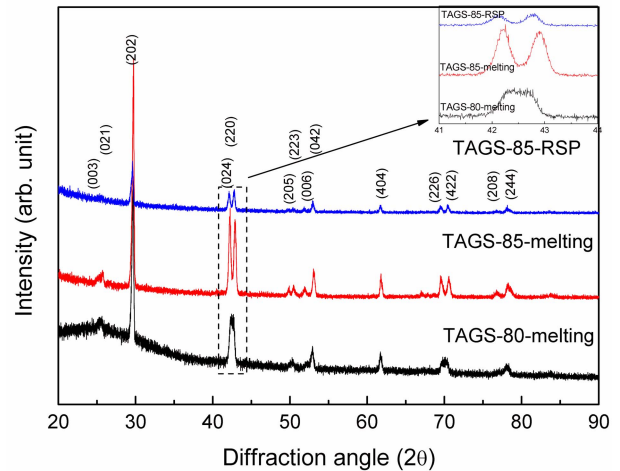


Fig. 2. XRD patterns of hot-pressed $(\text{GeTe})_x(\text{AgSbTe}_2)_{1-x}$ ($x = 80, 85$) compounds.

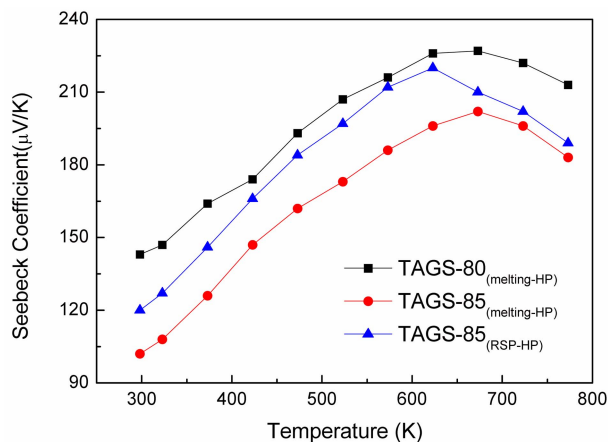
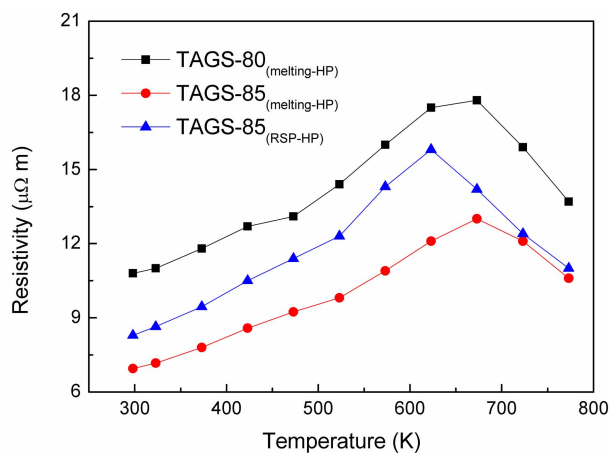
each specimen were shifted compared with the binary GeTe phase. The GeTe phase can be identified by the presence of (024) and (220) peaks.^[9] The inset of Fig. 2 shows the detailed diffraction angle (2θ : 41–44). In TAGS-80, the (024) and (220) peaks did not separate completely, but complete separation occurred in TAGS-85. In case of the TAGS compounds having higher Ag and Sb contents, the (024) and (220) peaks were not separated. Inversely, in compounds with lower contents of AgSbTe_2 , the two peaks were separated more clearly. The (024) peak was shifted to lower angle, but the (220) peak was shifted to higher angle.

From the XRD analysis of TAGS-85 produced by the RSP-hot press process, its phase was nearly crystalline in spite of rapidly solidified. This result will be detailed with HRTEM microstructure and discussed further in the latter part of this study. Table 1 shows the calculated lattice constants of hot-pressed TAGS- x ($x = 80, 85$) compounds. The lattice constant “ a ” was decreased, but the constant “ c ” increased with the contents of AgSbTe_2 increased. While the lattice constants of the TAGS-85 compounds produced with the melting-hot press process and the melting-RSP were nearly identical, but there was a difference between the lattice constants of TAGS-85 and 80 in the melting-hot press process. This shows that the changes in the lattice constant of TAGS compounds were affected by the compositions rather than fabrication process. The systematic change of x in TAGS- x compounds shows that GeTe and AgSbTe_2 behaved as solid solutions.^[12,13]

Figure 3 shows the temperature dependency of the Seebeck coefficient of hot-pressed TAGS- x compounds. The Seebeck coefficient of all specimens is positive through the measured temperature range, which means that TAGS- x compounds behave as a p-type semiconductor and the hole acts as a major carrier. The value of the Seebeck coefficient at the measured temperature range was about 102 $\mu\text{V/K}$ to

Table 1. Calculated lattice constant of hot pressed (GeTe)_x(AgSbTe₂)_{1-x} (x = 80, 85) compounds

Lattice constant	TAGS-85(RSP)	TAGS-85(melting)	TAGS-80(melting)
a (Å)	8.453±0.008	8.45±0.01	8.34±0.03
c (Å)	10.55±0.03	10.55±0.02	10.69±0.06

**Fig. 3.** Temperature dependency of Seebeck coefficient of TAGS-x (x = 80, 85) compounds.**Fig. 4.** Temperature dependency of electrical resistivity of TAGS-x (x = 80, 85) compounds.

227 $\mu\text{V/K}$. The Seebeck coefficient of all specimens increased in RT~650 K, but decreased at higher temperatures. The maximum Seebeck coefficient was 227 $\mu\text{V/K}$ at 673 K in TAGS-80 fabricated by the melting-HP process. The temperature dependency change of the Seebeck coefficient around 623 K was due to the phase transition from rhombohedral at room temperature to NaCl cubic structure at high temperature.^[6,13] TAGS compounds have a positive Seebeck coefficient and behaved as p-type semiconductors because the carrier is an Ag-site vacancy. The scattering between carriers becomes stronger with increasing carrier concentrations. And the Ag-site vacancy acts as potential carrier scattering site. These strong carrier-carrier scatterings can constrain carrier transport and reduce the Hall mobility in bulk specimens.^[14] In melting-hot press process, the Seebeck coefficient of TAGS-80 is higher than that of TAGS-85. The Seebeck coefficient of TAGS-85 by the RSP-hot press process is higher than that of TAGS-85 by melting-hot press. Thus, the Seebeck coefficient increased due to an increase in the amount of AgSbTe₂, and also by the RSP-hot press process.

Figure 4 shows the temperature dependency of electrical resistivity of hot-pressed TAGS-x compounds. TAGS-85 fabricated by melting-hot press shows the best electrical conductivity. The electrical resistivity was increased with increasing temperature in RT~650 K, but then decreased at over 650 K. Semiconducting behavior, which was highly degenerated under 650 K, could be discerned at 650 K or higher. The discontinuity in resistivity was measured in the whole specimen, owing to the phase transition of TAGS

compounds. This result coincided well with the results of temperature dependency of the Seebeck coefficient, as shown in Fig. 3, due to the transition from rhombohedral to NaCl cubic structure.^[13] The resistivity of TAGS-80 was higher than that of TAGS-85 in the melting-hot press process, which shows that the resistivity of TAGS-x decreased as the contents of Ag and Sb increased. In TAGS-85 compounds, the resistivity of the RSP-hot pressed specimen was higher than that of the melting-hot press specimen. Because the matrix of the RSP-hot pressed specimen has some amorphous phase which were not fully transformed to crystal structures, the resistivity increased in the matrix with the amorphous phase adjoined.^[15] Figure 5 shows the microstructure and selected area electron diffraction (SAED) pattern of the rapidly solidified TAGS-85 powder before hot-press, showing both amorphous and crystal structures. From the resulting change in resistivity, we can recognize that the electrical conductivity was affected by both compositions and fabrication process.

Table 2 shows the measured carrier concentration of the hot-pressed TAGS-x compounds. The values of the carrier concentration of TAGS-x were a sequence of TAGS-80_(melting-HP), TAGS-85_(RSP-HP) and TAGS-85_(melting-HP). The carrier concentrations of TAGS-x compounds were about 10^{20-21} , which is a difference of an order 1 to 2 magnitude compared with Bi-Te thermoelectric compounds, for which the carrier concentration is about 10^{19} . The relatively high carrier concentration of GeTe over Bi-Te-based thermoelectric compounds is because of the semimetallic behavior and nearly zero band gap of the GeTe compounds.^[16] As the car-

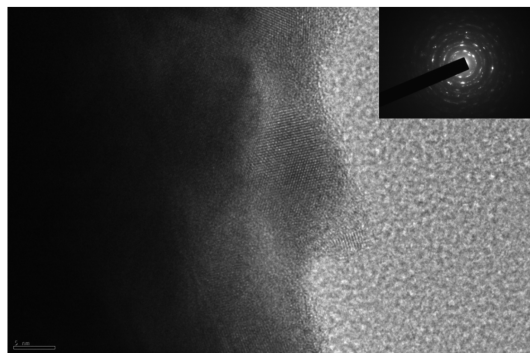


Fig. 5. TEM microstructure and SAED pattern of rapid solidified TAGS-85 powder.

Table 2. Carrier concentration of hot-pressed TAGS- x ($x = 80, 85$) compounds

specimen	carrier concentration (cm^{-3})
TAGS-80 _(melting-HP)	1.05×10^{20}
TAGS-85 _(melting-HP)	1.56×10^{21}
TAGS-85 _(RSP-HP)	3.95×10^{20}

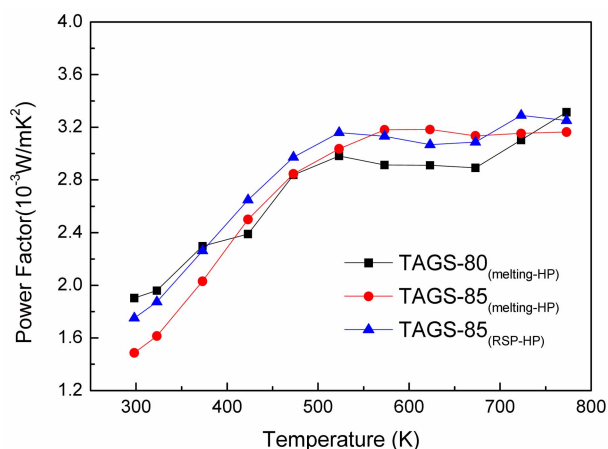


Fig. 6. Temperature dependency of power factor of TAGS- x ($x = 80, 85$) compounds.

rier concentration increases, both the Seebeck coefficient and resistivity decrease. The results of carrier concentration shown in Table 2 coincide well with the results of the Seebeck coefficient and resistivity change as shown in Figs. 3 and 4.

The power factor was calculated from the results of the Seebeck coefficient and the resistivity of TAGS- x compounds. Figure 5 shows the temperature dependency of the power factor (α^2/ρ) of TAGS- x ($x = 80, 85$) compounds. However, the difference in power factor was within nearly 10% of its value, which shows that no large difference occurs in power factor by the difference of compositions and/or fabrication processes. Thus we can estimate that the

performance of TAGS- x compounds will be affected primarily by the thermal conductivity. Other methods for the crystallization of amorphous materials were suggested such as homogeneous nucleation, crystallization quenched-in nuclei, and crystallization preceded by spinodal decomposition.^[17-19] However, the intensive studies of amorphous materials, their mechanisms in thermoelectric materials have hardly proceeded yet.

Further studies of the microstructure of the hot-pressed specimen, as well as the thermal conductivity composed with the lattice contribution (κ_{lat}) and the electronic contribution (κ_{e}) will be needed to clearly elucidate the effect of amorphous structures fabricated by the rapid solidification process.

4. CONCLUSIONS

We fabricated TAGS- x ($x = 80, 85$) thermoelectric compounds by melting-hot press and RSP-hot press processes to study the effect of compositions and non-crystalline structure. TAGS- x compounds were GeTe single phase. The electron transport properties of TAGS- x compounds were measured, and studied at RT~773 K to determine the effects of both composition and fabrication process, with particular focus given to the amorphous structure. The electron transport properties of TAGS-85 formed by the RSP-hot press process were located in the medium range of the TAGS-80 and TAGS-85 compounds by the melting-hot press. The best Seebeck coefficient was 227 $\mu\text{V/K}$ at 673 K in TAGS-80 fabricated by the melting-hot press process. The minimum resistivity was shown in the melting-hot pressed specimen of TAGS-85.

ACKNOWLEDGEMENT

This research was supported by a grant from the Fundamental R&D Program for Core Technology of Materials funded by the Ministry of Knowledge Economy, Republic of Korea.

REFERENCES

1. F. Ioffe, *Semiconductor Thermoelements and Thermoelectric Refrigeration*, p. 39, Infosearch, London (1957).
2. B. C. Sales, D. Mandrus, and R. K. Williams, *Science* **272**, 1325 (1996).
3. R. Venkatasubramanian, E. Siivola, T. Colpitts, and B. O'Quinn, *Nature* **413**, 597 (2001).
4. T. C. Harman, P. J. Taylor, M. P. Walsh, and B. E. LaForge, *Science* **297**, 2229 (2002).
5. K. F. Hsu, S. Loo, F. Guo, W. Chen, J. S. Dyck, C. Uher, T. Hogan, E. K. Polychroniadis, and M. G. Kanatzidis, *Science* **303**, 818 (2004).

6. E. A. Skrabek, and D. S. Trimmer, *CRC Handbook of Thermoelectrics* (ed., D. M. Rowe), pp. 267-275, CRC, Boca Raton, FL (1995).
7. G. C. Christakudis, S. K. Plachkova, L. E. Shelimova, and E. Avilov, *Phys. Status Solidi. A* **128**, 4652 (1991).
8. B. A. Cook, M. J. Kramer, X. Wei, and J. L. Haringa, *J. Appl. Phys.* **101**, 053715 (2007).
9. S. H. Yang, T. J. Zhu, T. Sun, J. He, S. N. Zhang, and X. B. Zhao, *Nanotechnology* **19**, 245707 (2008).
10. M. Zhou, J. F. Li, and T. Kita, *J. Am. Chem. Soc.* **130**, 4527 (2008).
11. B. Poudel, Q. Hao, Y. Ma, Y. Lan, A. Minnich, B. Yu, X. Yan, D. Wang, A. Muto, D. Vashaee, X. Chen, J. Liu, M. S. Dresselhaus, G. Chen, and Z. Ren, *Science* **320**, 634 (2008).
12. X. B. Zhao, X. H. Ji, Y. H. Zhang, T. J. Zhu, J. P. Tu, and X. B. Zhang, *Appl. Phys. Lett.* **86**, 062111 (2005).
13. J. R. Salvador, J. Yang, X. Shi, H. Wang, and A. A. Wereszczak, *J. Solid State Chem.* **182**, 2088 (2009).
14. S. H. Yang, T. J. Zhu, S. N. Zhang, J. J. Shen, and X. B. Zhao, *J. Electro. Mater.*, DOI: 10.1007/s11664-009-0993-y (2009).
15. J. L. Cui, H. Fu, X. L. Liu, D. Y. Chen, and W. Yang, *Curr. Appl. Phys.* **9**, 1170 (2009).
16. A. H. Edwards, A. C. Pineda, P. A. Schultz, M. G. Martin, A. P. Thompson, H. P. Hjalmarson, and C. J. Umrigar, *Phys. Rev. B* **73**, 045210 (2006).
17. P. Rizzi, C. Antonione, M. Barrico, L. Battezzati, L. Armelao, E. Tondello, M. Fabrizio, and S. Daolio, *Nanostruct. Mater.* **10**, 767 (1998).
18. J. H. Perepezko, R. J. Herbert, and G. Wilde, *Mater. Sci. Eng. A* **375-377**, 171 (2004).
19. K. F. Kelton, T. K. Croat, A. K. Gangopadhyay, L. Xing, and A. L. Greer, *J. Non-Cryst. Solids* **317**, 71 (2003).